Catalysis Today 146 (2009) 274–278

Contents lists available at ScienceDirect

Catalysis Today

journal homepage: www.elsevier.com/locate/cattod

# Oxygen storage in $O_2$/Pt/YSZ cell

Cyril Falgairette *, György Fóti

*Ecole Polytechnique Fédérale de Lausanne (EPFL), Institute of Chemical Sciences and Engineering, CH-1015 Lausanne, Switzerland*

ARTICLE INFO

*Article history:*
Available online 3 August 2009

*Keywords:*
EPOC
P-EPOC
Permanent promotion
Pt catalyst
Oxygen storage
Platinum oxide growth

ABSTRACT

The phenomenon of electrochemical promotion of catalysis (EPOC) was initially characterized as fully reversible, i.e. the catalyst restores its initial activity after current interruption. However, it has been recently demonstrated that after prolonged anodic polarization an unusual promoted activity is observed for a certain time after current interruption. This phenomenon has been reported as permanent electrochemical promotion of catalysis (P-EPOC).

In this work the oxygen storage reported as responsible of P-EPOC has been investigated by transient electrochemical techniques using an $O_2$(g)Pt/YSZ cell. A model has been proposed involving place interchange of Pt and O species in Pt/YSZ system. This seems to be induced by the strong lateral interaction of Pt–O surface dipoles and by increasing electric field at the Pt/YSZ interface. Such a rearranged oxide, so-called "phase oxide" can have a lower free energy than the initial monolayer oxide. This cooperative interaction of Pt and O species can lead to further thickening of this "phase oxide" especially at high temperature and potentials (currents). Furthermore, as the charge involved in this oxide thickening shows a $t^{1/2}$ dependency, the process seems to be diffusion controlled.



## 1. Introduction

Electrochemical promotion of catalysis (EPOC) denotes electrochemically controlled modification of heterogenous catalytic activity and selectivity. This phenomenon discovered by Vayenas et al. [1] has made a strong impact on solid state electrochemistry, catalysis and surface science. The EPOC phenomenon has been initially characterized as reversible, i.e. the catalyst restores its initial activity after current interruption [2,3]. Indeed, this is the case for short polarization times (few minutes). However, it has been demonstrated in our laboratory that after prolonged polarization (few hours) of the catalyst/YSZ interface, an unusual promoted activity is observed for a certain time after current interruption. This intriguing phenomenon, observed with $IrO_2$ [4], $RuO_2$ [5], Rh [6] and Pt [7,8] catalysts, is known as permanent electrochemical promotion of catalysis (P-EPOC). It has been reported that the phenomenon is linked to oxygen storage at different locations of the catalyst Pt/YSZ system during a prolonged anodic polarization [9]. This stored oxygen is believed to act as sacrificial promoter after current interruption [10].

In this work oxygen storage in the Pt/YSZ system has been investigated in a wide temperature range (425–550 °C) by means of different electrochemical techniques like cyclic voltammetry, chronoamperometry, chronopotentiometry and chronocoulometry using the $O_2$(g),Pt/YSZ cell. These techniques have been widely applied in liquid electrochemistry for the investigation of the Pt/liquid electrolyte interface, however, their application to solid state electrochemistry is very scarce [11–13].

## 2. Experimental

A three-electrode electrochemical cell was used. All three electrodes were platinum films deposited onto a 1.3 mm thick YSZ pellet (yttria-stabilized zirconia 8 mol%) by screen-printing of a paste, composed of 65 wt% of 1 μm particle size YSZ (8 mol% $Y_2O_3$ in $ZrO_2$, Tosoh) and 24% of a polyvinyl pyrrolidone solution (2% in isopropanol, Fluka), followed by sintering at 1400 °C in air to give a film thickness of 15 μm. Working, counter and reference electrodes, having a geometrical surface area of 0.08 $cm^2$ each, are composed of 62 vol% of platinum and 38 vol% of YSZ. This single-pellet three-electrode cell was suspended in a single-chamber type reactor with three gold wires serving as electrical contacts to the electrodes. A K-type (NiCr–Ni) thermocouple placed in proximity of the surface of the working electrode was used to measure the temperature of the system. The reactor was put into a furnace (XVA271, Horst) equipped with a heat control system (HT30, Horst). A mass flow controller (E-5514-FA, Bronkhorst) was used to keep the gas flow constant at 200 ml/min. The gas source was a Carbagas certified standard of $O_2$ (99.95%) supplied as a 20% mixture in He (99.996%). All the electrochemical measurements and data acquisition were made using a scanning potentiostat (Autolab, Model PGSTAT30, EcoChemie).

* Corresponding author. Tel.: +41 216936164.
*E-mail address:* cyril.falgairette@epfl.ch (C. Falgairette).

0920-5861/$ – see front matter © 2009 Elsevier B.V. All rights reserved.
doi:10.1016/j.cattod.2009.05.004

Before each electrochemical measurement, the cell has been pretreated by cathodic polarization at −600 mV for 10 min, this is in order to assure the same initial electrode state before measurements.

As both working (W) and reference (R) electrodes are in contact with the same gas composition (20 kPa $O_2$), the measured potential difference between the W and R electrode gives directly the electrode overpotential ($\eta$) at the working electrode.

## 3. Results and discussion

### 3.1. Chronoamperometric measurements

Fig. 1 shows chronoamperometric curves obtained at different anodic overpotentials ($\eta_a$). Initially the current decreases ($t < 10$ s) then starts to increase reaching a maximum (10 s $< t <$ 100 s). This maximum seems to be visible only for high overpotentials application ($\eta_a > 0.2$ V). For longer polarization ($t > 100$ s) the current reaches a steady state value which depends on the applied overpotential.

Furthermore, Fig. 1 shows that the time involved between starting potential application and the appearance of the current peak (lag time $t_{lag}$) decreases as the applied potential increases. The appearance of a current peak in the chronoamperometric measurements is a strong indication of sites regeneration, on the YSZ/Pt system, induced by the anodic polarization.

### 3.2. Chronopotentiometric measurements

Fig. 2 shows chronopotentiometric curves obtained at different applied anodic currents ($I_a$). For short times ($t < 10$ s) and for all applied currents ($I_a$) the potential increases rapidly with time. At intermediate times (10 s $< t <$ 50 s), the potential starts decreasing reaching a minimum value which is visible only for high $I_a$ (>300 mA). At longer times ($t > 50$ s) the potential starts to increase again reaching a steady value. The potential minimum observed at intermediate times in the chronopotentiometric measurements can be related with the liberation of new sites, as discussed in the chronoamperometric measurements.

Fig. 3 shows double step chronopotentiometric curves: application of an anodic current of 30 μA for a given holding time ($t_h$) followed by application of a cathodic current of −30 μA for the same holding time $t_h$.

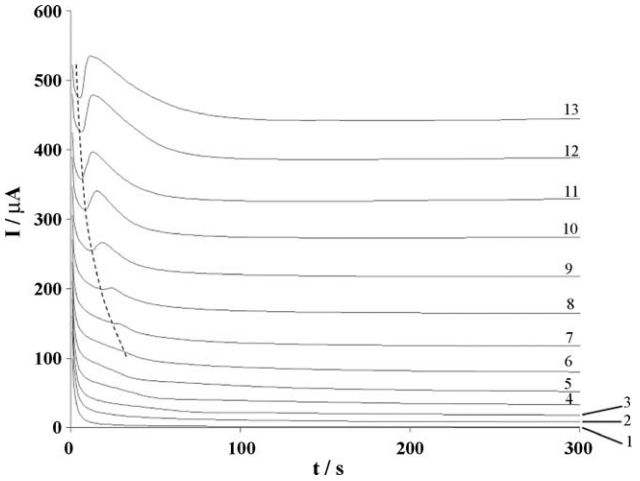


**Fig. 1.** Chronoamperometric curves obtained at various anodic overpotentials $\eta_a$. Increasing overpotential step of 50 mV from open circuit (1) to 600 mV (13), $T$ = 450 °C; $P_{O_2}$ = 20 kPa. Dashed line represents the evolution of lag time before the onset of the Pt site regeneration.

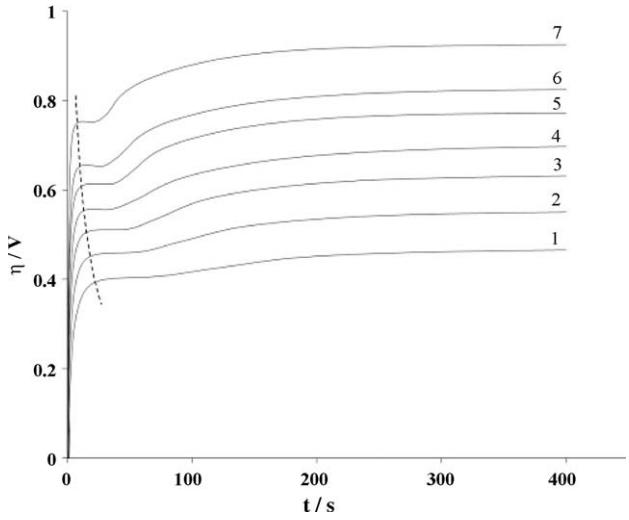


**Fig. 2.** Chronopotentiometric curves obtained at various applied anodic current $I_a$. Increasing anodic current step of 50 μA from 300 μA (1) to 600 μA (7), $T$ = 450 °C; $P_{O_2}$ = 20 kPa. Dashed line represents the evolution of lag time before the onset of the Pt site regeneration.

The anodic chronopotentiometric curves show a single plateau even after polarization as long as 1000 s, however, the cathodic chronopotentiometric curves shows at least two shoulders which are visible only for high anodic holding times ($t_h > 200$ s).

### 3.3. Chronocoulometric measurements

This is a two step process: in the first step, a constant anodic overpotential ($\eta_a$) was applied on to the $O_2$(g)Pt/YSZ cell for varying holding times (charging of the cell). In the second step a constant cathodic overpotential ($\eta_c$) was applied for 150 s (discharging of the cell). During discharging, the current ($I$) passing through the cell was recorded as a function of time ($t$) as is shown in Fig. 4a for the case of $\eta_a$ = 100 mV and $\eta_c$ = 300 mV at $T$ = 450 °C. From this figure the involved stored charge ($Q_{stor}$) has been determined by integration, taking the discharging curve obtained after 5 min as base line.

Fig. 5 shows $Q_{stor}$ as a function of anodic holding time ($t_h$) at 100 mV and the inset shows the dependence of $Q_{stor}$ on $t_h^{1/2}$. The

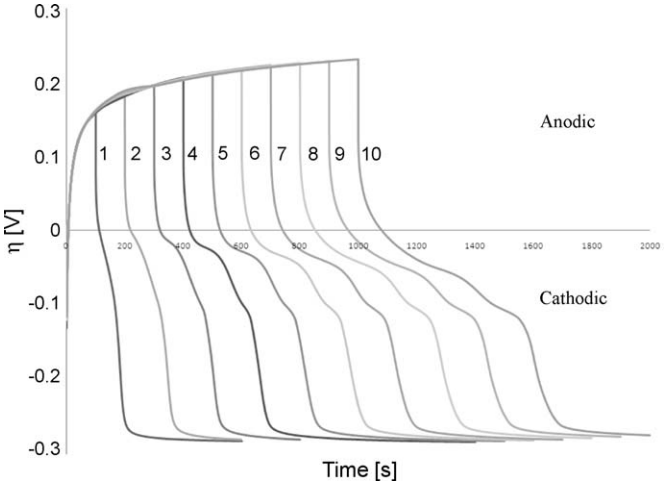


**Fig. 3.** Double step chronopotentiometry of the $O_2$(g), Pt/YSZ system. An anodic current ($I_a$ = 30 μA) is applied during 10 different holding times, from 100 s (1) to 1000 s (10), followed by application of a cathodic current ($I_c$ = −30 μA) during 1000 s. $P_{O_2}$ = 20 kPa, $T$ = 475 °C.

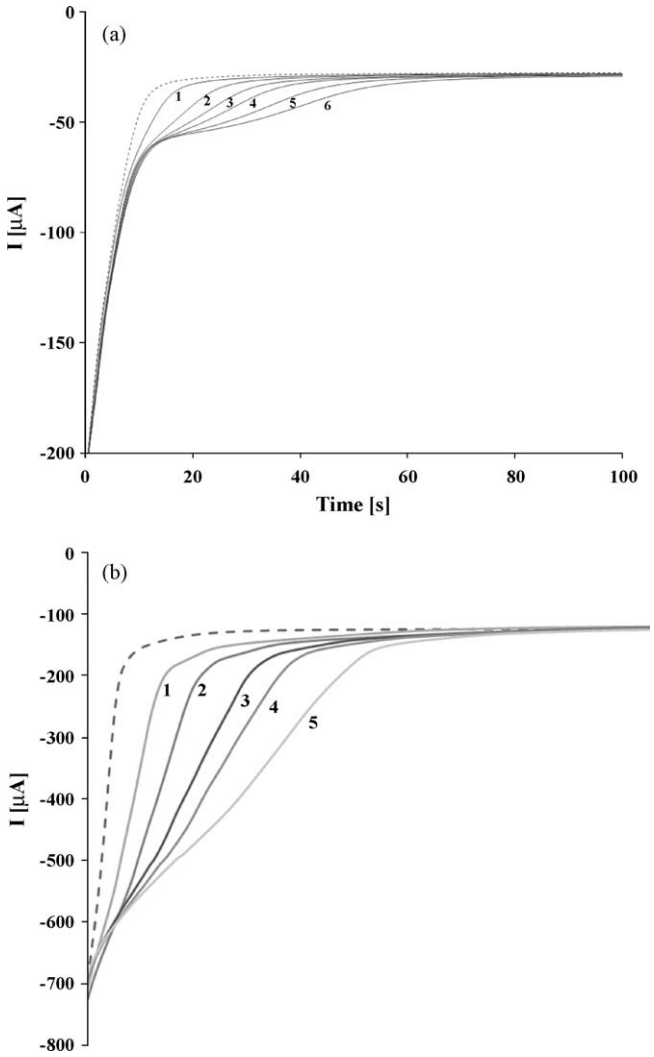


**Fig. 4.** Double step chronoamperometric measurements. *I–t* transients obtained during the discharging step. Influence of the holding time $t_h$ at a given anodic overpotential. (a) Curves labeled 1–6 refer to holding times of 10, 20, 30, 40, 60 and 80 min, respectively; $\eta_a = 100$ mV, $\eta_c = -300$ mV, $P_{O_2} = 20$ kPa, $T = 450$ °C. (b) Curves labeled 1–5 refer to holding times of 5, 10, 20, 30 and 60 min, respectively; $\eta_a = 200$ mV, $\eta_c = -600$ mV, $P_{O_2} = 20$ kPa, $T = 475$ °C. Dashed line shows the baseline used for peak area integration.

linear dependence of $Q_{stor}$ on $t_h^{1/2}$ indicates that we are dealing with a slow charging process suggesting a diffusion mechanism.

Similar results have been obtained working at higher temperature (475 °C), higher applied anodic overpotentials ($\eta_a = 200$ mV) and higher cathodic overpotentials ($\eta_c = -600$ mV), mV), as it is shown in Fig. 4b.

### 3.4. Voltammetric measurements

Fig. 6a shows typical voltammetric responses (10 mV/s) of the $O_2$(g)Pt/YSZ cell after anodic polarization at 100 mV for different holding times $t_h$ ($T = 450$ °C). At short holding times (few minutes) two distinct reduction peaks appear, as has been reported by others [1]. However, for $t_h$ longer than 15 min a third peak clearly appears and its area increases with increasing holding time. The electrical charges ($Q_1$, $Q_2$ and $Q_3$) involved in the three peaks, numbered in order of increasing cathodic peak potential, were determined by peak integration and are reported as equivalent amounts of oxygen atoms ($N_1$, $N_2$ and $N_3$) calculated with the exchange of two electrons. Fig. 7 shows that both $N_1$ and $N_2$ reach

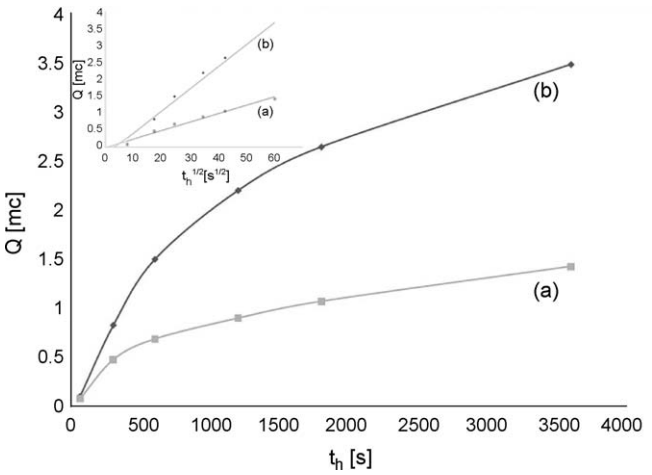


**Fig. 5.** Effect of the holding time $t_h$ on charge storage, dependence with time and dependence with the square root of time in the inset. (a) $\eta_a = 100$ mV, $\eta_c = -300$ mV, $P_{O_2} = 20$ kPa, $T = 450$ °C. (b) $\eta_a = 200$ mV, $\eta_c = -600$ mV, $P_{O_2} = 20$ kPa, $T = 475$ °C.

rapidly saturation indicating that there is a limited number of free sites for the process related to these two peaks. The situation is different for $N_3$ which grows continuously without any tendency for saturation even after 2000 min of anodic polarization at 100 mV. $N_3$ shows some interesting feature. In fact, it shows a lag time of about 5 min (inset of Fig. 7) and seems to start growing only when $N_1$ has reached saturation. Furthermore, the charge related

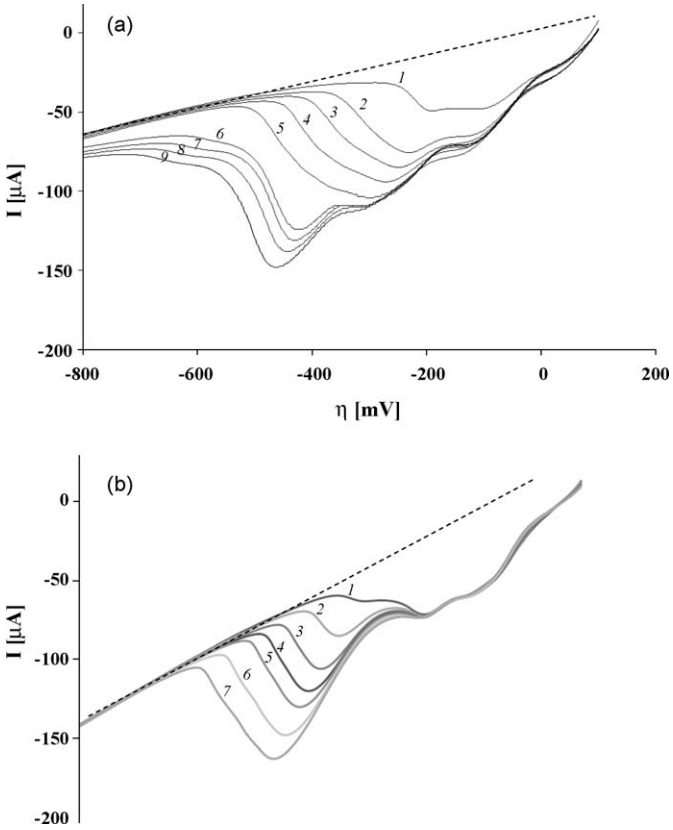


**Fig. 6.** Linear sweep voltammetry in the $O_2$(g),Pt/YSZ system. Effect of the holding time, $t_h$, at $\eta_h = 100$ mV on the first cathodic scan. (a) Curves labeled 1–9 refer to holding times of 0, 5, 10, 20, 30, 80, 100, 120 and 200 min, respectively; $T = 450$ °C, $P_{O_2} = 20$ kPa, $\nu = 10$ mV/s. (b) Curves labeled 1–7 refer to holding times of 10, 30, 60, 90, 120, 180 and 240 min, respectively; $T = 475$ °C, $P_{O_2} = 20$ kPa, $\nu = 20$ mV/s. Dashed line shows the baseline used for peak area integration.

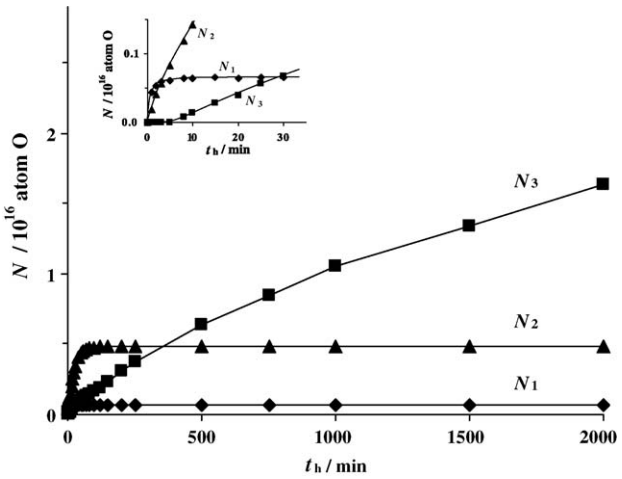


**Fig. 7.** Amount of stored oxygen related to the 1st, 2nd and 3rd peaks of Fig. 6a. The amount of oxygen atoms, *N*, is calculated assuming the exchange of two electrons. The inset shows a zoom on the domain of short holding time [9].

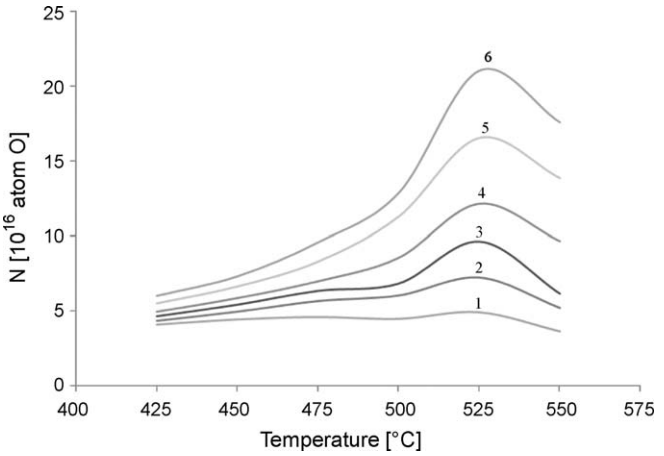


**Fig. 9.** Effect of temperature on the total amount of stored oxygen calculated from the voltammetric measurements. Curves 1–6 refer to holding times of 30, 60, 90, 120, 180 and 240 min at $\eta_h$ = 100 mV, $P_{O_2}$ = 20 kPa, $\nu$ = 10 mV $s^{-1}$. The amount of stored oxygen, *N*, is calculated assuming the exchange of two electrons.

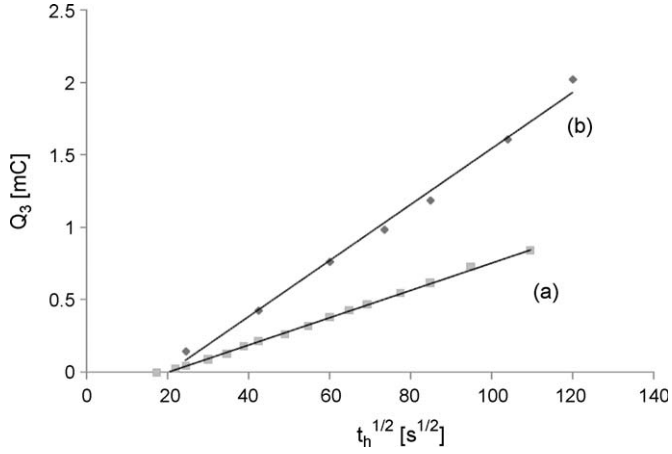


**Fig. 8.** Plot of the charge relative to the third peak ($Q_3$) of voltammograms of Fig. 6 as a function of the square root of time. (a) $T$ = 450 °C, $P_{O_2}$ = 20 kPa, $\eta_h$ = 100 mV, $\nu$ = 10 mV/s. (b) $T$ = 475 °C, $P_{O_2}$ = 20 kPa, $\eta_h$ = 100 mV, $\nu$ = 20 mV/s.

with this peak ($Q_3$) has a $t^{1/2}$ dependency (Fig. 8), this is again an indication that diffusion is involved in the charging process related with the 3rd peak.

The voltammetric measurements of the $O_2$(g)Pt/YSZ cell have been also carried out at different temperatures in the region between 425 and 550 °C. The general feature of the obtained responses is similar to that shown in Fig. 6b obtained at 475 °C. However, a distinct separation of the three peaks is much more difficult at low (425 °C) and high (550 °C) temperatures. Furthermore, it has been found that the total storage capacity ($N_1 + N_2 + N_3$) of the Pt/YSZ system increases with temperature reaching a maximum at about 525 °C then it decreases with increasing temperature (Fig. 9). The observed decrease of charging capacity above the critical temperature of 525 °C is certainly related with the thermal stability of platinum oxide. In fact, the reported dissociation temperature ($T_{dis}$) of platinum oxide is 535 °C at $P_{O_2}$ = 21 kPa [18]. In case of our system we expect a higher dissociation temperature than that calculated considering bulk oxygen partial pressure, and this is due to local increase (at the Pt/YSZ) of $P_{O_2}$ induced by the reaction of oxygen evolution and due to trapping of $O_2$ as reported by Janek et al. [17].

## 4. General discussion

As has been discussed in a previous paper [10] the three peaks observed in the voltammetric measurements (Fig. 8a) correspond to stored oxygen present at three significantly different locations of the Pt/YSZ system. Furthermore, it has been postulated [7,9,10] that stored oxygen species related to the 2nd peak are involved in EPOC and those related to the 3rd peak are responsible for the P-EPOC phenomenon. This can relate the lag time observed for the 3rd peak in the electrochemical measurements with the need of prolonged polarization time in order to observe the P-EPOC.

A reaction scheme involving platinum oxidation (reduction) (Eq. (1)) and oxygen evolution (reduction) (Eq. (2)) is proposed to take place in parallel during the anodic (cathodic) polarization of the Pt/YSZ interface in $O_2$ atmosphere.

$$Pt + xO^{2-} \rightleftarrows PtO_x + 2xe^- \quad (1)$$

$$2O^{2-} \rightleftarrows O_2(g) + 4e^- \quad (2)$$

Oxygen evolution (Eq. (2)) is the main process during anodic polarization, however, platinum oxide formation (Eq. (1)) seems to influence the kinetics of $O^{2-}$ discharge. In fact, chronoamperometric technique used in this work shows clearly that under anodic overpotential application the responding current firstly decreases, and then it increases to reach a maximum before decreasing again to a steady state (see Fig. 1). Mutatis mutandis, the same is valid for chronopotentiometric experiments, where the overpotential response to a current application firstly increases, and then it decreases to reach a minimum before increasing again to a steady state (see Fig. 2). The time constant involved in the initial decrease of activity for $O^{2-}$ discharge is of a few seconds. The involved amount of stored oxygen is about $7 \times 10^{14}$ O atoms (see Fig. 7). This storage is supposed to be due to the formation of platinum oxide layer at the Pt/YSZ interface and at the three phase boundaries (tpb) Pt–YSZ–$O_2$ [10]. This oxide seems to act as a barrier for the oxygen evolution reaction inducing electron transfer through the film by tunnelling. It is worthwhile to mention at this stage that double layer charging, which have a time constant of few milliseconds, are neglected during our transient measurements. The subsequent increase in activity for $O^{2-}$ discharge observed at longer polarization times is certainly related with the liberation of free sites induced by the applied anodic overpotential or current. The minimum of activity observed after a given lag time can be

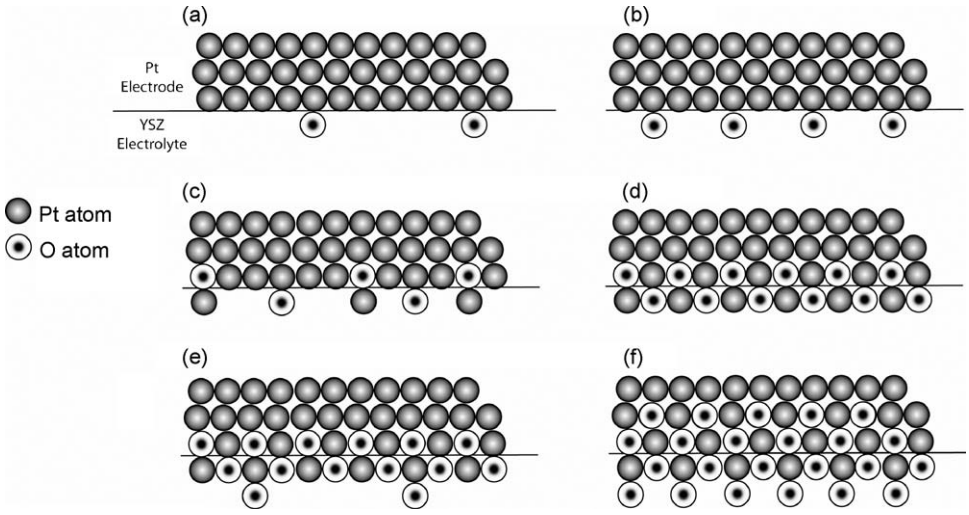


**Fig. 10.** Schematic representation of the platinum oxide growth mechanism in a $O_2$(g) Pt/YSZ cell: (a) electrosorbed oxygen; (b) critical coverage of electrosorbed oxygen at Pt/YSZ interface; (c) surface rearrangement of Pt and O species with regeneration of Pt active sites; (d) first complete layer of platinum oxide; (e) and (f) are the following steps leading to "phase oxide".

explained by the fact that the liberation of active sites takes place after having reached a given critical surface coverage of the electrode surface by electrosorbed oxygen (platinum oxide).

Considering a similar mechanism as for Pt in contact with aqueous electrolyte [11–13] we can speculate that this regeneration occurs via surface rearrangement processes involving place interchange of Pt and O species as shown schematically in Fig. 10. This is induced by the strong lateral interaction of Pt–O surface dipoles and by increasing electric field at the Pt/YSZ interface.

Such a rearranged oxide, so-called "phase oxide" can have a lower free energy than the initial monolayer oxide and consequently it is thermodynamically more stable. This accounts for the more negative reduction potential of the 3rd peak observed in the voltammetric measurements (Fig. 6). This cooperative interaction of Pt and O species can lead to further thickening of this "phase oxide" especially at high temperature and with high overpotentials (currents). In fact, our results have shown that oxygen storage increases with increasing applied overvoltage (current) and by increasing temperature in the region of the thermodynamic stability of platinum oxide. Furthermore, as the charge involved in this oxide thickening shows a $t^{1/2}$ dependency, the process seems to be diffusion controlled.

It must be mentioned that the germ of the idea of surface oxide rearrangement in aqueous electrolyte originated in the work of Schuldiner and Warner [14] who had proposed in a qualitative way that anodically electrosorbed oxygen species were in some kind of "dermasorbed state", i.e. in the skin of the metal surface.

## 5. Conclusion

The effect of anodic polarization of a platinum electrode deposited on YSZ solid electrolyte was studied in $O_2$-containing atmosphere by electrochemical methods. Transient techniques revealed that oxygen evolution is the main process during anodic polarization, however, platinum oxide formation seems to influence the kinetics of $O^{2-}$ discharge. A model has been proposed for the oxygen storage in a $O_2$(g)/Pt/YSZ cell involving place interchange of Pt and O species. This seems to be induced by the strong lateral interaction of Pt–O surface dipoles and by increasing electric field at the Pt/YSZ interface. Such a rearranged oxide, so-called "phase oxide", is speculated to be responsible of the permanent EPOC phenomenon.

## Acknowledgement

Financial support from the *Fonds National Suisse de la Recherche Scientifique* is gratefully acknowledged.

## References

[1] C.G. Vayenas, S. Bebelis, C. Pliangos, S. Brosda, D. Tsiplakides, Electrochemical Activation of Catalysis: Promotion, Electrochemical Promotion and Metal-Support Interactions, Kluwer Academic/Plenum Publishers, New York, 2001.
[2] C.G. Vayenas, S. Bebelis, S. Neophitides, J. Phys. Chem. 92 (1988) 5083.
[3] C.G. Vayenas, S. Bebelis, S. Ladas, Nature 343 (1990) 625.
[4] J. Nicole, D. Tsiplakides, S. Wodiunig, Ch. Comninellis, J. Electrochem. Soc. 144 (1997) L312.
[5] S. Wodiunig, V. Patsis, Ch. Comninellis, Solid State Ionics 136 (2000) 813.
[6] G. Foti, O. Lavanchy, Ch. Comninellis, J. Appl. Electrochem. 30 (2000) 1223.
[7] A. Jaccoud, G. Foti, R. Wüthrich, H. Jotterand, Ch. Comninellis, Top. Catal. 44 (2007) 409.
[8] S. Balomenou, G. Pitselis, D. Polydoros, A. Giannikos, A. Vradis, A. Frenzel, C. Panglios, H. Putter, C.G. Vayenas, Solid State Ionics 136 (2000) 857.
[9] A. Jaccoud, C. Falgairette, G. Foti, Ch. Comninellis, Electrochim. Acta 52 (2007) 7927.
[10] C. Falgairette, A. Jaccoud, G. Foti, Ch. Comninellis, J. Appl. Electrochem. 38 (2008) 1075.
[11] H. Angerstein-Kozlowska, B. MacDougall, B.E. Conway, J. Electrochem. Soc. 120 (1973) 756.
[12] S.J. Xia, V.I. Birss, Electrochim. Acta 45 (2000) 3659.
[13] G. Jerkiewicz, G. Vatankhah, J. Lessard, M.P. Soriaga, Y. Park, Electrochim. Acta 49 (2004) 1451.
[14] S. Schuldiner, T.B. Warner, J. Electrochem. Soc. 112 (1965) 212.